

Charmed-strange Meson Spectrum: Old and New Problems

Jorge Segovia,^{*} David R. Entem,[†] and Francisco Fernández[‡]

*Grupo de Física Nuclear and Instituto Universitario de Física Fundamental y Matemáticas (IUFFyM)
Universidad de Salamanca, E-37008 Salamanca, Spain*

(Dated: November 6, 2018)

The LHCb Collaboration has recently reported the observation for the first time of a spin-3 resonance in the heavy quark sector. They have shown that the $\bar{D}^0 K^-$ structure seen in the $B_s^0 \rightarrow \bar{D}^0 K^- \pi^+$ reaction and with invariant mass 2.86 GeV is an admixture of a spin-1 and a spin-3 resonances. Motivated by the good agreement between our theoretical predictions some time ago and the properties extracted from the experiment of the $D_{s1}^*(2860)$ and $D_{s3}^*(2860)$ states, we perform an extension of the study of the strong decay properties of the $D_{sJ}^*(2860)$ and present the same analysis for the $D_{s1}^*(2700)$ and $D_{sJ}(3040)$ mesons. This provides a unified and simultaneous description of the three higher excited charmed-strange resonances observed until now. For completeness, we present theoretical results for masses and strong decays of the low-lying charmed-strange mesons and those experimental missing states which belong to the spin-multiplets of the discovered $D_{s1}^*(2700)$, $D_{sJ}^*(2860)$ and $D_{sJ}(3040)$ resonances. The theoretical framework used is a constituent quark model which successfully describes hadron phenomenology from light to heavy quark sectors.

PACS numbers: 12.39.-x, 14.40.Lb

Keywords: Quark models, charmed mesons.

I. INTRODUCTION

The spectrum of charmed-strange mesons contains a number of well established states [1] corresponding to the S -wave D_s and D_s^* mesons with spin-parity 0^- and 1^- , respectively; and the P -wave states with quantum numbers $J^P = 0^+$ ($D_{s0}^*(2317)$), 1^+ ($D_{s1}(2460)$ and $D_{s1}(2536)$) and 2^+ ($D_{s2}^*(2573)$).

In addition, between the years 2006 and 2009, three new $c\bar{s}$ mesons were observed at the B -factories in DK and D^*K decay modes and in three-body b -hadron decays [2–4]. These states have been recently included in the Particle Data Group (PDG) as the $D_{s1}^*(2700)$, the $D_{sJ}^*(2860)$ and the $D_{sJ}(3040)$. While the $D_{s1}^*(2700)$ is commonly believed to have quantum numbers $J^P = 1^-$, there are several possibilities for the $D_{sJ}^*(2860)$ and $D_{sJ}(3040)$ states. Different predictions of the theoretical models can be found in Refs. [5–8].

Recent experiments performed by the LHCb Collaboration have contributed to clarify the puzzle around the $D_{sJ}^*(2860)$ resonance [9, 10]. A careful re-examination of the $\bar{D}^0 K^-$ invariant mass around 2.86 GeV in the decay $B_s^0 \rightarrow \bar{D}^0 K^- \pi^+$ finds that a spin-1 state and a spin-3 state overlap under the peak. Since the resonance substructure of the three-body decay is analysed through a Dalitz plot, the well-defined initial state allows to unambiguously determine the quantum numbers, in particular, the parity of the $D_{sJ}^*(2860)$ state to be odd. The determined masses and widths of the $D_{s1}^*(2860)$ and $D_{s3}^*(2860)$

are [9, 10]

$$\begin{aligned} M(D_{s1}^*(2860)) &= (2859 \pm 12 \pm 6 \pm 23) \text{ MeV}, \\ \Gamma(D_{s1}^*(2860)) &= (159 \pm 23 \pm 27 \pm 72) \text{ MeV}, \end{aligned} \quad (1)$$

and

$$\begin{aligned} M(D_{s3}^*(2860)) &= (2860.5 \pm 2.6 \pm 2.5 \pm 6.0) \text{ MeV}, \\ \Gamma(D_{s3}^*(2860)) &= (53 \pm 7 \pm 4 \pm 6) \text{ MeV}, \end{aligned} \quad (2)$$

where the first uncertainty is statistical, the second is systematic and the third is due to model variations.

Spin-3 states had never been observed in heavy flavoured mesons and so these new measurements have led to many theoretical works [11–16]. In Ref. [17] we predicted two resonances 1^3D_1 and 1^3D_3 at 2.86 GeV with total decay widths 153 MeV and 85 MeV, respectively¹.

Motivated by the excellent agreement with the LHCb results, we will address in this work an extension of our study to all strong decay properties of the $D_{sJ}^*(2860)$ resonance. Moreover, we will present the same analysis for the $D_{s1}^*(2700)$ and $D_{sJ}(3040)$ mesons. We will work within the framework of a constituent quark model (CQM) proposed in Ref. [18] (see references [19] and [20] for reviews). This model successfully describes hadron phenomenology and hadronic reactions [21–23] and has recently been applied to mesons containing heavy quarks (see, for instance, Refs. [24–27]).

For completeness, we will resume our theoretical results for the masses of the low-lying charmed-strange mesons and calculate strong decays for those states above

^{*} segonza@usal.es

[†] entem@usal.es

[‡] fdz@usal.es

¹ Note that we are using here spectroscopic notation: $n^{2S+1}L_J$, where n refers to the radial excitation with $n = 1$ indicating the ground state, and S , L and J is the spin-, angular- and total-momentum of the $c\bar{s}$ pair.

the open-flavour threshold, the $D_{s1}(2536)$ and $D_{s2}^*(2573)$ mesons. There are $c\bar{s}$ states which have not yet been seen by experiments but belong to the spin-multiplets of the discovered $D_{s1}^*(2700)$, $D_{sJ}^*(2860)$ and $D_{sJ}(3040)$ resonances. We will also compute their masses and strong decay properties in order to guide experimentalists in their search.

This manuscript is arranged as follows. In Sec. II we will describe the main properties of the constituent quark model relevant to the heavy quark sector and review the 3P_0 strong decay model adapted to our formalism. In Sec. III we will present our theoretical results. First, we will review our quark model results for the properties of the low-lying charmed-strange mesons; second, we will compare the available experimental data of the $D_{s1}^*(2700)$, $D_{sJ}^*(2860)$ and $D_{sJ}^*(3040)$ resonances with the theoretical predictions attending to our quantum number assignments. And third, we will compute masses and strong decay properties of those states that are experimentally missing and lie in the same energy range of the $D_{s1}^*(2700)$, $D_{sJ}^*(2860)$ and $D_{sJ}^*(3040)$ resonances. Partial decay widths into all open-decay channels will be provided in order to guide experimentalists in the quest of completing the information of the charmed-strange meson sector. We will summarize and give some conclusions in Sec. IV.

II. THEORETICAL FRAMEWORK

A. The constituent quark model

Spontaneous chiral symmetry breaking of the QCD Lagrangian together with the perturbative one-gluon exchange (OGE) and the nonperturbative confining interaction are the main pieces of constituent quark models. Using this idea, Vijande *et al.* [18] developed a model of the quark-quark interaction which is able to describe meson phenomenology from the light to the heavy quark sector.

The wide energy range needed to provide a consistent description of light, strange and heavy mesons requires an effective scale-dependent strong coupling constant. We use the frozen coupling constant [18]

$$\alpha_s(\mu) = \frac{\alpha_0}{\ln\left(\frac{\mu^2 + \mu_0^2}{\Lambda_0^2}\right)}, \quad (3)$$

in which μ is the reduced mass of the $q\bar{q}$ pair and α_0 , μ_0 and Λ_0 are parameters of the model determined by a global fit to the meson spectra.

In the heavy quark sector chiral symmetry is explicitly broken and Goldstone-boson exchanges do not appear. Thus, OGE and confinement are the only interactions remaining. The one-gluon exchange potential contains central, tensor and spin-orbit contributions given by

$$\begin{aligned} V_{\text{OGE}}^{\text{C}}(\vec{r}_{ij}) &= \frac{1}{4}\alpha_s(\vec{\lambda}_i^c \cdot \vec{\lambda}_j^c) \left[\frac{1}{r_{ij}} - \frac{1}{6m_i m_j} (\vec{\sigma}_i \cdot \vec{\sigma}_j) \frac{e^{-r_{ij}/r_0(\mu)}}{r_{ij} r_0^2(\mu)} \right], \\ V_{\text{OGE}}^{\text{T}}(\vec{r}_{ij}) &= -\frac{1}{16} \frac{\alpha_s}{m_i m_j} (\vec{\lambda}_i^c \cdot \vec{\lambda}_j^c) \left[\frac{1}{r_{ij}^3} - \frac{e^{-r_{ij}/r_g(\mu)}}{r_{ij}} \left(\frac{1}{r_{ij}^2} + \frac{1}{3r_g^2(\mu)} + \frac{1}{r_{ij} r_g(\mu)} \right) \right] S_{ij}, \\ V_{\text{OGE}}^{\text{SO}}(\vec{r}_{ij}) &= -\frac{1}{16} \frac{\alpha_s}{m_i^2 m_j^2} (\vec{\lambda}_i^c \cdot \vec{\lambda}_j^c) \left[\frac{1}{r_{ij}^3} - \frac{e^{-r_{ij}/r_g(\mu)}}{r_{ij}^3} \left(1 + \frac{r_{ij}}{r_g(\mu)} \right) \right] \times \\ &\quad \times \left[((m_i + m_j)^2 + 2m_i m_j) (\vec{S}_+ \cdot \vec{L}) + (m_j^2 - m_i^2) (\vec{S}_- \cdot \vec{L}) \right], \end{aligned} \quad (4)$$

where $r_0(\mu) = \hat{r}_0 \frac{\mu_{nn}}{\mu_{ij}}$ and $r_g(\mu) = \hat{r}_g \frac{\mu_{nn}}{\mu_{ij}}$ are regulators which depend on μ_{ij} , the reduced mass of the $q\bar{q}$ pair. The contact term of the central potential has been regularized as

$$\delta(\vec{r}_{ij}) \sim \frac{1}{4\pi r_0^2} \frac{e^{-r_{ij}/r_0}}{r_{ij}}. \quad (5)$$

One characteristic of the model is the use of a screened linear confinement potential. This has been able to reproduce the degeneracy pattern observed for the higher excited states of light mesons [28]. As we assume that confining interaction is flavour independent, we hope that this form of the potential will be useful in our case

because we are focusing on the high energy region of the charmed-strange meson spectrum.

The different pieces of the confinement potential are

$$\begin{aligned} V_{\text{CON}}^{\text{C}}(\vec{r}_{ij}) &= [-a_c(1 - e^{-\mu_c r_{ij}}) + \Delta] (\vec{\lambda}_i^c \cdot \vec{\lambda}_j^c), \\ V_{\text{CON}}^{\text{SO}}(\vec{r}_{ij}) &= -(\vec{\lambda}_i^c \cdot \vec{\lambda}_j^c) \frac{a_c \mu_c e^{-\mu_c r_{ij}}}{4m_i^2 m_j^2 r_{ij}} \times \\ &\quad \times \left[((m_i^2 + m_j^2)(1 - 2a_s) \right. \\ &\quad \left. + 4m_i m_j(1 - a_s)) (\vec{S}_+ \cdot \vec{L}) \right. \\ &\quad \left. + (m_j^2 - m_i^2)(1 - 2a_s) (\vec{S}_- \cdot \vec{L}) \right]. \end{aligned} \quad (6)$$

where a_s controls the mixture between the scalar and vector Lorentz structures of the confinement. At short

Quark masses	m_n (MeV)	313
	m_s (MeV)	555
	m_c (MeV)	1763
	m_b (MeV)	5110
	OGE	\hat{r}_0 (fm)
	\hat{r}_g (fm)	0.259
	α_0	2.118
	Λ_0 (fm ⁻¹)	0.113
	μ_0 (MeV)	36.976
Confinement	a_c (MeV)	507.4
	μ_c (fm ⁻¹)	0.576
	Δ (MeV)	184.432
	a_s	0.81

TABLE I. Quark model parameters.

distances this potential presents a linear behaviour with an effective confinement strength $\sigma = -a_c \mu_c (\vec{\lambda}_i^c \cdot \vec{\lambda}_j^c)$, while it becomes constant at large distances. This type of potential shows a threshold defined by

$$V_{\text{thr}} = \{-a_c + \Delta\} (\vec{\lambda}_i^c \cdot \vec{\lambda}_j^c). \quad (7)$$

No $q\bar{q}$ bound states can be found for energies higher than this threshold.

Table I shows the model parameters used herein. Further details about the quark model and the fine-tuned model parameters can be found in Refs. [18, 24, 28].

Among the different methods to solve the Schrödinger equation in order to find the quark-antiquark bound states, we use the Gaussian Expansion Method [29] which provides enough accuracy and it simplifies the subsequent evaluation of the decay amplitude matrix elements.

This procedure provides the radial wave function solution of the Schrödinger equation as an expansion in terms of basis functions

$$R_\alpha(r) = \sum_{n=1}^{n_{max}} c_n^\alpha \phi_{nl}^G(r), \quad (8)$$

where α refers to the channel quantum numbers. The coefficients, c_n^α , and the eigenvalue, E , are determined from the Rayleigh-Ritz variational principle

$$\sum_{n=1}^{n_{max}} \left[(T_{n'n}^\alpha - EN_{n'n}^\alpha) c_n^\alpha + \sum_{\alpha'} V_{n'n}^{\alpha\alpha'} c_n^{\alpha'} = 0 \right], \quad (9)$$

where $T_{n'n}^\alpha$, $N_{n'n}^\alpha$ and $V_{n'n}^{\alpha\alpha'}$ are the matrix elements of the kinetic energy, the normalization and the potential, respectively. $T_{n'n}^\alpha$ and $N_{n'n}^\alpha$ are diagonal, whereas the mixing between different channels is given by $V_{n'n}^{\alpha\alpha'}$.

Following Ref. [29], we employ Gaussian trial functions with ranges in geometric progression. This enables the optimization of ranges employing a small number of free parameters. Moreover, the geometric progression is dense at short distances, so that it enables the description of the dynamics mediated by short range potentials. The fast damping of the Gaussian tail does not represent an issue, since we can choose the maximal range much longer than the hadronic size.

The model described above is not able to reproduce the spectrum of the P -wave charmed-strange mesons. The inconsistency with experiment is mainly due to the fact that the mass splittings between the $D_{s0}^*(2317)$, $D_{s1}(2460)$ and $D_{s1}(2536)$ mesons are not well reproduced. The same problem appears in Lattice QCD calculations [30] or other quark models [31].

In order to improve these mass splittings we follow the proposal of Ref. [32] and include one-loop corrections to the OGE potential as derived by Gupta *et al.* [33]. This correction shows a spin-dependent term which affects only mesons with different flavour quarks.

The net result is a quark-antiquark interaction that can be written as:

$$V(\vec{r}_{ij}) = V_{\text{OGE}}(\vec{r}_{ij}) + V_{\text{CON}}(\vec{r}_{ij}) + V_{\text{OGE}}^{1\text{-loop}}(\vec{r}_{ij}), \quad (10)$$

where V_{OGE} and V_{CON} were defined before and are treated non-perturbatively. $V_{\text{OGE}}^{1\text{-loop}}$ is the one-loop correction to OGE potential which is treated perturbatively. As in the case of V_{OGE} and V_{CON} , $V_{\text{OGE}}^{1\text{-loop}}$ contains central, tensor and spin-orbit contributions given by [32]

$$V_{\text{OGE}}^{1\text{-loop,C}}(\vec{r}_{ij}) = 0,$$

$$V_{\text{OGE}}^{1\text{-loop,T}}(\vec{r}_{ij}) = \frac{C_F}{4\pi} \frac{\alpha_s^2}{m_i m_j} \frac{1}{r^3} S_{ij} \left[\frac{b_0}{2} \left(\ln(\mu r_{ij}) + \gamma_E - \frac{4}{3} \right) + \frac{5}{12} b_0 - \frac{2}{3} C_A \right. \\ \left. + \frac{1}{2} \left(C_A + 2C_F - 2C_A \left(\ln(\sqrt{m_i m_j} r_{ij}) + \gamma_E - \frac{4}{3} \right) \right) \right],$$

$$\begin{aligned}
V_{OGE}^{1\text{-loop,SO}}(\vec{r}_{ij}) &= \frac{C_F}{4\pi} \frac{\alpha_s^2}{m_i^2 m_j^2} \frac{1}{r^3} \times \\
&\times \left\{ (\vec{S}_+ \cdot \vec{L}) \left[((m_i + m_j)^2 + 2m_i m_j) (C_F + C_A - C_A (\ln(\sqrt{m_i m_j} r_{ij}) + \gamma_E)) \right. \right. \\
&\quad \left. \left. + 4m_i m_j \left(\frac{b_0}{2} (\ln(\mu r_{ij}) + \gamma_E) - \frac{1}{12} b_0 - \frac{1}{2} C_F - \frac{7}{6} C_A + \frac{C_A}{2} (\ln(\sqrt{m_i m_j} r_{ij}) + \gamma_E) \right) \right. \right. \\
&\quad \left. \left. + \frac{1}{2} (m_j^2 - m_i^2) C_A \ln \left(\frac{m_j}{m_i} \right) \right] \right. \\
&\quad \left. + (\vec{S}_- \cdot \vec{L}) \left[(m_j^2 - m_i^2) (C_F + C_A - C_A (\ln(\sqrt{m_i m_j} r_{ij}) + \gamma_E)) \right. \right. \\
&\quad \left. \left. + \frac{1}{2} (m_i + m_j)^2 C_A \ln \left(\frac{m_j}{m_i} \right) \right] \right\}, \tag{11}
\end{aligned}$$

where $C_F = 4/3$, $C_A = 3$, $b_0 = 9$, $\gamma_E = 0.5772$ and the scale $\mu \sim 1 \text{ GeV}$.

B. The 3P_0 Decay model

Meson strong decay is a complex nonperturbative process that has not yet been described from first principles of QCD. Several phenomenological models have been developed to deal with this topic. The most popular is the 3P_0 model [34–36] which assumes that a quark-antiquark pair is created with vacuum quantum numbers, $J^{PC} = 0^{++}$.

An important characteristic, apart from its simplicity, is that the model provides the gross features of various transitions with only one parameter, the strength γ of the decay interaction. Some attempts have been done to find possible dependences of the vertex parameter γ , see [37] and references therein. In Ref. [17] we performed a global fit to the decay widths of the mesons which belong to charmed, charmed-strange, hidden charm and hidden bottom sectors and elucidated the dependence on the mass scale of the 3P_0 free parameter γ . Further details about the global fit can be found in Ref. [17]. The running of the strength γ of the 3P_0 decay model is given by

$$\gamma(\mu) = \frac{\gamma_0}{\log\left(\frac{\mu}{\mu_0}\right)}, \tag{12}$$

where μ is the reduced mass of the quark-antiquark in the decaying meson and, $\gamma_0 = 0.81 \pm 0.02$ and $\mu_0 = (49.84 \pm 2.58) \text{ MeV}$ are parameters determined by the global fit.

We get a quite reasonable global description of the total decay widths in all meson sectors, from light to heavy. All the wave functions for the mesons involved in the open-flavour strong decays are the solutions of the Schrödinger equation with the potential model described above and using the Gaussian Expansion Method [29]. Details of the resulting matrix elements for different cases

are given in Ref. [38], here we proceed to explain briefly the main ingredients in which the model is based.

1. Transition operator

The interaction Hamiltonian involving Dirac quark fields that describes the production process is given by

$$H_I = \sqrt{3} g_s \int d^3x \bar{\psi}(\vec{x}) \psi(\vec{x}), \tag{13}$$

where we have introduced for convenience the numerical factor $\sqrt{3}$, which will be cancelled with the color factor.

If we write the Dirac fields in second quantization and keep only the contribution of the interaction Hamiltonian which creates a $(\mu\nu)$ quark-antiquark pair, we arrive, after a nonrelativistic reduction, to the following expression for the transition operator

$$\begin{aligned}
T &= -\sqrt{3} \sum_{\mu,\nu} \int d^3p_\mu d^3p_\nu \delta^{(3)}(\vec{p}_\mu + \vec{p}_\nu) \frac{g_s}{2m_\mu} \sqrt{2^5 \pi} \times \\
&\times \left[\mathcal{Y}_l \left(\frac{\vec{p}_\mu - \vec{p}_\nu}{2} \right) \otimes \left(\frac{1}{2} \frac{1}{2} \right) 1 \right]_0 a_\mu^\dagger(\vec{p}_\mu) b_\nu^\dagger(\vec{p}_\nu), \tag{14}
\end{aligned}$$

where μ (ν) are the spin, flavour and color quantum numbers of the created quark (antiquark). The spin of the quark and antiquark is coupled to one. The $\mathcal{Y}_{lm}(\vec{p}) = p^l Y_{lm}(\hat{p})$ is the solid harmonic defined in function of the spherical harmonic.

As in Ref. [39], we fix the relation of g_s with the dimensionless constant giving the strength of the quark-antiquark pair creation from the vacuum as $\gamma = g_s/2m$, being m the mass of the created quark (antiquark). In this convention, values of the scale-dependent strength γ in the different quark sectors following Eq. (12) can be found in Ref. [17]. We use herein the one corresponding to the charmed-strange meson sector: $\gamma = 0.38$.

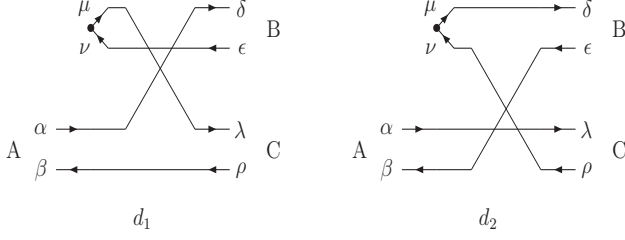


FIG. 1. Diagrams that can contribute to the decay width through the 3P_0 model.

2. Transition amplitude

We are interested on the transition amplitude for the reaction $(\alpha\beta)_A \rightarrow (\delta\epsilon)_B + (\lambda\rho)_C$. The meson A is formed by a quark α and antiquark β . At some point it is created a $(\mu\nu)$ quark-antiquark pair. The created $(\mu\nu)$ pair together with the $(\alpha\beta)$ pair in the original meson regroups in the two outgoing mesons via a quark rearrangement process. These final mesons are meson B which is formed by the quark-antiquark pair $(\delta\epsilon)$ and

meson C with $(\lambda\rho)$ quark-antiquark pair.

We work in the center-of-mass reference system of meson A , thus we have $\vec{K}_A = \vec{K}_0 = 0$ with \vec{K}_A and \vec{K}_0 the total momentum of meson A and of the system BC with respect to a given reference system. We can factorize the matrix element as follow

$$\langle BC|T|A\rangle = \delta^{(3)}(\vec{K}_0)\mathcal{M}_{A\rightarrow BC}. \quad (15)$$

The initial state in second quantization is

$$|A\rangle = \int d^3p_\alpha d^3p_\beta \delta^{(3)}(\vec{K}_A - \vec{P}_A) \phi_A(\vec{p}_A) a_\alpha^\dagger(\vec{p}_\alpha) b_\beta^\dagger(\vec{p}_\beta) |0\rangle, \quad (16)$$

where α (β) are the spin, flavour and color quantum numbers of the quark (antiquark). The wave function $\phi_A(\vec{p}_A)$ denotes a meson A in a color singlet with an isospin I_A with projection M_{I_A} , a total angular momentum J_A with projection M_A , J_A is the coupling of angular momentum L_A and spin S_A . The \vec{p}_α and \vec{p}_β are the momentum of quark and antiquark, respectively. The \vec{P}_A and \vec{p}_A are the total and relative momentum of the $(\alpha\beta)$ quark-antiquark pair within the meson A . The final state is more complicated than the initial one because it is a two-meson state. It can be written as

$$\begin{aligned} |BC\rangle &= \frac{1}{\sqrt{1 + \delta_{BC}}} \int d^3K_B d^3K_C \sum_{m, M_{BC}} \langle J_{BC} M_{BC} l m | J_T M_T \rangle \delta^{(3)}(\vec{K} - \vec{K}_0) \delta(k - k_0) \\ &\frac{Y_{lm}(\hat{k})}{k} \sum_{M_B, M_C, M_{I_B}, M_{I_C}} \langle J_B M_B J_C M_C | J_{BC} M_{BC} \rangle \langle I_B M_{I_B} I_C M_{I_C} | I_A M_{I_A} \rangle \\ &\int d^3p_\delta d^3p_\epsilon d^3p_\lambda d^3p_\rho \delta^{(3)}(\vec{K}_B - \vec{P}_B) \delta^{(3)}(\vec{K}_C - \vec{P}_C) \\ &\phi_B(\vec{p}_B) \phi_C(\vec{p}_C) a_\delta^\dagger(\vec{p}_\delta) b_\epsilon^\dagger(\vec{p}_\epsilon) a_\lambda^\dagger(\vec{p}_\lambda) b_\rho^\dagger(\vec{p}_\rho) |0\rangle, \end{aligned} \quad (17)$$

where we have followed the notation of meson A for the mesons B and C . We assume that the final state of mesons B and C is a spherical wave with angular momentum l . The relative and total momentum of mesons B and C are \vec{k}_0 and \vec{K}_0 . The total spin J_{BC} is obtained coupling the total angular momentum of mesons B and C , and J_T is the coupling of J_{BC} and l .

The 3P_0 model takes into account only diagrams in which the $(\mu\nu)$ quark-antiquark pair separates into different final mesons. This was originally motivated by the experiment and it is known as the Okubo-Zweig-Iizuka (OZI)-rule [40–42] which tells us that the disconnected diagrams are more suppressed than the connected ones. The diagrams that can contribute to the decay width through the 3P_0 model are shown in Fig. 1.

3. Decay width

The total width is the sum over the partial widths characterized by the quantum numbers J_{BC} and l

$$\Gamma_{A\rightarrow BC} = \sum_{J_{BC}, l} \Gamma_{A\rightarrow BC}(J_{BC}, l), \quad (18)$$

where

$$\Gamma_{A\rightarrow BC}(J_{BC}, l) = 2\pi \int dk_0 \delta(E_A - E_{BC}) |\mathcal{M}_{A\rightarrow BC}(k_0)|^2. \quad (19)$$

We use relativistic phase space, so

$$\Gamma_{A\rightarrow BC}(J_{BC}, l) = 2\pi \frac{E_B(k_0) E_C(k_0)}{m_A k_0} |\mathcal{M}_{A\rightarrow BC}(k_0)|^2, \quad (20)$$

	D_s	D_s^*	$D_{s0}^*(2317)$	$D_{s1}(2460)$	$D_{s1}(2536)$	$D_{s2}(2573)$
This work (α_s)	1984	2110	2510	2593	2554	2591
This work (α_s^2)	1984	2104	2383	2570	2560	2609
Experiment	1969.0 ± 1.4	2112.3 ± 0.5	2318.0 ± 1.0	2459.6 ± 0.9	2535.18 ± 0.24	2571.9 ± 0.8

TABLE II. Masses, in MeV, of the low-lying charmed-strange mesons predicted by the constituent quark model (α_s) and those including one-loop corrections to the OGE potential (α_s^2). Experimental data are taken from Ref. [1].

where

$$k_0 = \frac{\sqrt{[m_A^2 - (m_B - m_C)^2][m_A^2 - (m_B + m_C)^2]}}{2m_A}, \quad (21)$$

is the on-shell relative momentum of mesons B and C .

III. RESULTS

A. Review of low-lying states

Table II shows the masses of the low-lying charmed-strange mesons predicted by the constituent quark model. One can see our results taking into account the one-gluon exchange potential (α_s) and including its one-loop corrections (α_s^2).

The theoretical masses for the D_s and D_s^* mesons agree with the experimental measurements. We also find a reasonable agreement for the $D_{s1}(2536)$ and $D_{s2}(2573)$ masses. The state assigned to the $D_{s0}^*(2317)$ is very sensitive to the one-loop corrections of the OGE potential which bring its mass closer to the experimental one. This effect could explain part of its lower mass as a $c\bar{s}$ state, but threshold effects should be taken into account before a definitive statement can be given about its nature. The spin dependent corrections to the OGE potential are not enough to solve the puzzle in the $1^+ c\bar{s}$ sector. In Ref. [25] we have studied the $J^P = 1^+$ charmed-strange channel, finding that the $D_{s1}(2460)$ has an important non- $q\bar{q}$ contribution whereas the $D_{s1}(2536)$ is almost a pure $q\bar{q}$ state. However, the presence of non- $q\bar{q}$ degrees of freedom modifies the $D_{s1}(2536)$ wave function in such way that explains most of its decay properties [25, 43, 44].

Table III shows the partial and total strong decay widths of the mesons $D_{s1}(2536)$ and $D_{s2}^*(2573)$. We show the absolute values in MeV and the branching fractions in %. One can see that the total decay widths reported by PDG [1] are in excellent agreement with our results. For the $D_{s1}(2536)$ meson, the PDG provides the following two-body decay branching ratios (concerning strong decays):

$$R_1 = \frac{\Gamma(D_{s1}(2536)^+ \rightarrow D^{*0}K^+)}{\Gamma(D_{s1}(2536)^+ \rightarrow D^{*+}K^0)} = 1.18 \pm 0.16,$$

$$R_2 = \frac{\Gamma(D_{s1}(2536)^+ \rightarrow D^{*+}K^0)}{\Gamma(D_{s1}(2536)^+ \rightarrow D^{*+}K^0)} = 0.72 \pm 0.05 \pm 0.01, \quad (22)$$

Meson	$n J^P$	Channel	Γ_{3P_0} (MeV)	\mathcal{B}_{3P_0} (%)	$\Gamma_{\text{exp.}}$ (MeV)
$D_{s1}(2536)^+$	$1 1^+$	$D^{*+}K^0$	0.43	43.48	
		$D^{*0}K^+$	0.56	56.52	
		total	0.99	100	0.92 ± 0.05
$D_{s2}(2573)^+$	$1 2^+$	D^+K^0	8.02	42.95	
		D^0K^+	8.69	46.54	
		$D^{*+}K^0$	0.82	4.40	
		$D^{*0}K^+$	1.06	5.67	
		$D_s^+\eta$	0.08	0.44	
total	18.67	100	17 ± 4		

TABLE III. Open-flavour strong decay widths, in MeV, and branching fractions, in %, of the $D_{s1}(2536)$ and $D_{s2}^*(2573)$ mesons. Experimental data are taken from Ref. [1].

which compare reasonably well with our theoretical results for $R_1 = 1.31$ and $R_2 = 0.66$. For $D_{s1}^*(2573)$ meson, the PDG only reports an upper limit on the ratio $D^{*0}K^+/D^0K^+$ of 0.33. Our theoretical figure 0.12 is compatible with such a limit. It is worth to mention here that in the work in which the LHCb Collaboration disentangles the resonance structure of the peak around 2.86 GeV [10], they also provide the $D_{s2}^*(2573)$ mass and width with significantly better precision than previous measurements

$$M(D_{s2}(2573)) = (2568.39 \pm 0.29 \pm 0.19 \pm 0.18) \text{ MeV},$$

$$\Gamma(D_{s2}(2573)) = (16.9 \pm 0.5 \pm 0.4 \pm 0.4) \text{ MeV}, \quad (23)$$

and both are in reasonable agreement with our theoretical results: 2.61 GeV and 18.67 MeV, respectively.

B. The $D_{s1}^*(2700)$ resonance

It is commonly believed that the $D_{s1}^*(2700)$ is the first excitation of the D_s^* meson. Our quark model predicts a mass in this energy range (2.79 GeV) but also for the $n^{2S+1}L_J = 2^1S_0$ state (2.73 GeV). However, if the $D_{s1}^*(2700)$ had quantum numbers $J^P = 0^-$ it would not decay into DK final state, and this is incompatible with the experimental observations. Table IV shows the open-flavour strong decays of the $D_{s1}^*(2700)$ meson as the 2^3S_1 state.

Meson	nJ^P	Channel	Γ_{3P_0} (MeV)	\mathcal{B}_{3P_0} (%)	$\Gamma_{\text{exp.}}$ (MeV)
$D_{s1}^*(2700)$	21^-	DK	36.99	21.67	
		D^*K	97.78	57.26	
		$D_s\eta$	3.67	2.15	
		$D_s^*\eta$	9.51	5.57	
		$D^*K_0^*$	22.80	13.35	
	total	170.75	100	125 ± 30	

TABLE IV. Open-flavour strong decay widths, in MeV, and branching fractions, in %, of the $D_{s1}^*(2700)$ meson with quantum numbers $nJ^P = 21^-$. Experimental data are taken from Ref. [1].

The total decay width of $D_{s1}^*(2700)$ as the 2^3S_1 state is slightly larger but close to the experimental value. The information of the partial decay widths shown in Table IV points out that the D^*K decay channel is dominant and the DK and $D^*K_0^*$ are important. In addition, the $D_{s1}^*(2700)$ meson has traces in $D_s\eta$ and $D_s^*\eta$ with partial widths of several MeV. Finally, our theoretical value for the branching ratio D^*K/DK is 2.6, which is a factor 3 larger than the experimental measurement $0.91 \pm 0.13 \pm 0.12$ reported by the BaBar Collaboration [4]. Similar discrepancies can be found in other quark models. This fact may be an indication of a bigger mixture between the 2^3S_1 and 1^3D_1 states [16]. In our model the mixing is not fitted to the experimental data but driven by the tensor piece of the quark-antiquark interaction. Our states are almost pure 3S_1 or 3D_1 in the $J^P = 1^-$ channel. It would be very helpful that the LHCb Collaboration, with significantly better precision than previous experiments, repeats the measurement of this ratio.

C. The $D_{sJ}^*(2860)$ resonance

According to the observed decay modes, the possible spin-parity quantum numbers of the $D_{sJ}^*(2860)$ are $J^P = 1^-, 2^+, 3^-$, and so on. The 2^+ assignment is disfavoured because it would be the excitation of the $D_{s2}^*(2573)$ meson and our model predicts a mass around 3.1 GeV. Beyond $J = 3$ the predicted masses are much higher than the experimental measurement. Table V shows the open-flavour strong decays of the $D_{sJ}^*(2860)$ as the third excitation of the 1^- meson (mostly dominated by the 1^3D_1 channel) and as the ground state of 3^- meson (mostly dominated by the 1^3D_3 channel).

The predicted total decay widths are in excellent agreement with the LHCb observation of having two resonances at 2.86 GeV, one of spin-1 and another one of spin-3. Table V shows that the DK , D^*K and DK^* decay channels are very important for the $D_{s1}^*(2860)$ meson. However, the $D_{s3}^*(2860)$ resonance decays mainly into DK , D^*K and $D^*K_0^*$ final states being the partial width into DK^* very small. We also observe that the

Meson	nJ^P	Channel	Γ_{3P_0} (MeV)	\mathcal{B}_{3P_0} (%)	$\Gamma_{\text{exp.}}$ (MeV)
$D_{sJ}^*(2860)$	31^-	DK	53.34	34.81	
		D^*K	38.43	25.08	
		$D_s\eta$	12.12	7.92	
		$D_s^*\eta$	5.06	3.30	
		$D^*K_0^*$	7.15	4.67	
	total	37.10	24.22		
	total	153.20	100	$159 \pm 23 \pm 27 \pm 72$	
$D_{sJ}^*(2860)$	13^-	DK	38.57	45.32	
		D^*K	26.17	30.74	
		$D_s\eta$	1.06	1.24	
		$D_s^*\eta$	0.35	0.41	
		$D^*K_0^*$	16.16	18.99	
	total	2.81	3.30		
	total	85.12	100	$53 \pm 7 \pm 4 \pm 6$	

TABLE V. Open-flavour strong decay widths, in MeV, and branching fractions, in %, of the $D_{sJ}^*(2860)$ meson with quantum numbers $nJ^P = 31^-$ or 13^- . Experimental data are taken from Refs. [9, 10]

$D_{s1}^*(2860)$ meson has traces in $D_s\eta$ and $D_s^*\eta$ while the partial decay widths of the $D_{s3}^*(2860)$ into these final states are very tiny. With respect the branching ratio measured by the BaBar Collaboration [4], we obtain

$$\frac{\mathcal{B}(D_{sJ}^*(2860) \rightarrow D^*K)}{\mathcal{B}(D_{sJ}^*(2860) \rightarrow DK)} = \begin{cases} 0.72 & D_{s1}^*(2860), \\ 0.68 & D_{s3}^*(2860), \end{cases} \quad (24)$$

which compares reasonably well with the experimental one, $1.10 \pm 0.15 \pm 0.19$. In view of our results, we cannot distinguish if the branching ratio measured by BaBar belongs to the $D_{s1}^*(2860)$ or to the $D_{s3}^*(2860)$. It would be again very helpful that the LHCb Collaboration repeats the measurement of this ratio.

D. The $D_{sJ}(3040)$ resonance

The mean $2P$ multiplet mass is predicted in our model to be 3.06 GeV which is near the mass of the $D_{sJ}(3040)$ resonance. Therefore, the possible assignments are the $J^P = 0^+$ which only decays into DK , the 1^+ which only decays into D^*K and the 2^+ which decays into DK and D^*K . The only decay mode in which $D_{sJ}(3040)$ has been seen until now is the D^*K , and so the most possible assignment is that the $D_{sJ}(3040)$ meson being the next excitation in the 1^+ channel.

Table VI shows the open-flavour strong decays of the $D_{sJ}(3040)$ meson as the $nJ^P = 31^+$ or 41^+ state. The mass of the $D_{sJ}(3040)$ is large enough to allow open-flavour strong decays not studied before in this work like the D^*K^* final state. In fact, this decay channel is dominant in both $nJ^P = 31^+$ and 41^+ states followed

Meson	nJ^P	Channel	Γ_{3P_0}	\mathcal{B}_{3P_0}	$\Gamma_{\text{exp.}}$	
$D_{sJ}(3040)$	$nJ^P = 31^+$	D^*K	25.22	8.36		
		DK_0^*	0.76	0.25		
		$D_s^*\eta$	3.26	1.08		
		$D^*K_0^*$	0.02	0.01		
		DK^*	44.28	14.69		
		$D_{s0}^*\eta$	0.97	0.32		
		D_0^*K	2.81	0.93		
		D^*K^*	156.78	52.00		
		D_1K	39.81	13.20		
		$D_1'K$	0.69	0.23		
		D_2^*K	11.19	3.71		
		$D_s\phi$	15.54	5.15		
		$D_{s1}(2460)\eta$	0.19	0.07		
		total		301.52	100	$239 \pm 35^{+46}_{-42}$
		$D_{sJ}(3040)$	$nJ^P = 41^+$	D^*K	53.48	12.37
DK_0^*	0.30			0.07		
$D_s^*\eta$	4.97			1.15		
$D^*K_0^*$	1.10			0.25		
DK^*	100.38			23.21		
$D_{s0}^*\eta$	1.66			0.38		
D_0^*K	2.31			0.53		
D^*K^*	130.91			30.27		
D_1K	11.58			2.68		
$D_1'K$	0.04			0.01		
D_2^*K	123.74			28.61		
$D_s\phi$	1.97			0.45		
$D_{s1}(2460)\eta$	0.09			0.02		
total				432.53	100	$239 \pm 35^{+46}_{-42}$

TABLE VI. Open-flavour strong decay widths, in MeV, and branching fractions, in %, of the $D_{sJ}(3040)$ meson with quantum numbers $nJ^P = 31^+$ or 41^+ . Experimental data are taken from Ref. [1].

by the DK^* in the case of the 31^+ and by the D_2^*K and DK^* in the case of the 41^+ . Moreover, the $nJ^P = 31^+$ state has partial decay widths in the order of tens of MeV for the D^*K , D_1K , $D_s\phi$ and D_2^*K decay channels; whereas for the $nJ^P = 41^+$ we find only partial widths in the order of tens of MeV for the D^*K and D_1K . Finally, the total decay widths are large for both states, being that of the $nJ^P = 31^+$ state in better agreement with the experimental data.

There are other two states which belong to the mean $2P$ multiplet that are still missing in experiment. These states are the first radial excitation of the $c\bar{s}$ mesons with quantum numbers $J^P = 0^+$ and 2^+ , respectively. The masses predicted by our model are 2.93 GeV for the $nJ^P = 20^+$ and 3.09 GeV for the 22^+ . These masses are in agreement with recent studies of the charmed-strange meson sector [13, 16]. It is worthy to remind here that the $J^P = 0^+$ channel is very sensitive to the 1-loop correction

Meson	nJ^P	Channel	Γ_{3P_0}	\mathcal{B}_{3P_0}		
$D_{s0}^*(2934)$	20^+	DK	60.62	32.67		
		$D_s\eta$	3.31	1.78		
		$D^*K_0^*$	4.47	2.41		
		D^*K^*	86.42	46.57		
		D_1K	18.43	9.93		
		$D_1'K$	0.14	0.08		
		$D_s\eta'$	12.17	6.56		
		total	185.56	100		
		$D_{s2}^*(3094)$	22^+	DK	2.14	0.95
				D^*K	1.90	0.84
$D_s\eta$	0.02			0.01		
$D_s^*\eta$	1.02			0.45		
$D^*K_0^*$	0.80			0.36		
DK^*	40.32			17.91		
D^*K^*	124.26			55.18		
D_1K	17.59			7.81		
$D_1'K$	6.35			2.82		
$D_s\eta'$	1.71			0.76		
D_2^*K	26.30	11.68				
$D_s\phi$	0.00	0.00				
$D_{s1}(2460)\eta$	2.44	1.09				
$D_0^*K_0^*$	0.32	0.14				
total	225.17	100				

TABLE VII. Open-flavour strong decay widths, in MeV, and branching fractions, in %, of the $nJ^P = 20^+$ and $nJ^P = 22^+$ states.

of the OGE potential. For the second excitation, its mass goes from 3.03 to 2.93 GeV.

Table VII shows their partial and total decay widths calculated with the 3P_0 decay model. The masses used for the initial mesons are the theoretical ones. There are less open decay channels for the $nJ^P = 20^+$ resonance than for the 22^+ . However, the total decay widths are very similar being 185.55 MeV and 225.17 MeV, respectively. The D^*K^* decay channel is dominant for the two resonances. One can also find traces of the D_1K decay channel in both cases, but the DK^* and D_2^*K decays are only important for the 22^+ resonance. It is remarkably that the 20^+ resonance has large partial width to DK whereas this is not the case for the 22^+ state. The authors of Ref. [16] predict the same behaviour than us and notice that there is an evidence of a structure around 2.96 GeV in the \bar{D}^0K^- invariant mass spectrum given by LHCb [9, 10] that can be associated to the 20^+ resonance.

E. The missing states around 2.86 GeV

We have assigned to the $D_{s1}^*(2700)$ meson the $nJ^P = 21^-$ state and to the $D_{sJ}^*(2860)$ meson the 31^- and

Meson	$n J^P$	Channel	Γ_{3P_0}	\mathcal{B}_{3P_0}
$D_s(2729)$	20^-	D^*K	190.62	66.81
		DK_0^*	87.41	30.64
		$D_s^*\eta$	7.28	2.55
		total	285.31	100
$D_{s2}(2888)$	12^-	D^*K	54.74	23.45
		DK_0^*	35.92	15.39
		$D_s^*\eta$	0.99	0.43
		$D^*K_0^*$	8.19	3.51
		DK^*	133.55	57.22
		$D_{s0}^*\eta$	0.00	0.00
		D_0^*K	0.00	0.00
		total	233.39	100
		$D_{s2}(2948)$	22^-	D^*K
DK_0^*	4.52			2.42
$D_s^*\eta$	19.10			10.22
$D^*K_0^*$	9.51			5.09
DK^*	31.61			16.92
$D_{s0}^*\eta$	0.00			0.00
D_0^*K	0.02			0.01
D^*K^*	36.30			19.42
D_1K	0.12			0.06
$D_1'K$	0.01			0.00
$D_s\eta'$	0.00			0.00
total	186.89			100

TABLE VIII. Open-flavour strong decay widths, in MeV, and branching fractions, in %, of the $nJ^P = 20^-$, $nJ^P = 12^-$ and $nJ^P = 22^-$ states.

13^- states. The last two assignments are based on the disentanglement of spin-1 and spin-3 resonances around the 2.86 GeV peak performed by the LHCb Collaboration [9, 10]. Around this energy range, there are still three states not seen by experiments. These are the second radial excitation of the charmed-strange ground state $nJ^P = 20^-$ and the 12^- and 22^- states which are the D -wave partners of the $D_{sJ}^*(2860)$ meson.

The masses predicted by our constituent quark model are 2.79 GeV, 2.89 GeV and 2.95 GeV for the $nJ^P = 20^-$, 12^- and 22^- , respectively. These masses are in agreement with Refs. [13, 16] except for the 20^- state which seems that our model predicts a mass slightly higher. Table VIII shows partial and total decay widths for the three states. One can see that we predict a 20^- state much broader than recent studies of the same states [13, 16]. There are two main reasons for this: i) our theoretical mass is different and this influences the calculation of the decay widths in the 3P_0 model; ii) Refs. [13, 16] do not calculate the partial width into the DK_0^* despite this decay channel is open for the mass they predict. The DK_0^* decay channel contributes 30% to the total decay width in our model and sum almost 100 MeV to it.

With respect the other two states, 12^- and 22^- , their masses and total decay widths are very similar to those predicted in Refs. [13, 16]. One can distinguish common features between their predictions and ours. The first one is that these states seems quite broad with total decay widths around 200 MeV. The second one is that the dominant decay channels for the 22^- state are D^*K , DK^* and D^*K^* with traces also in the $D_s^*\eta$. However, there are also differences. The relative order in the dominant channels for the 22^- state is different and, what is more important, our predictions for the partial decay widths of the $nJ^P = 12^-$ seems quite different. They predict that its dominant decay channel is D^*K followed by the $D_s^*\eta$ whereas we have a dominant DK^* followed by the D^*K and DK_0^* decay channels.

IV. SUMMARY AND CONCLUSIONS

We have performed an extensive study of strong decay properties for the $D_{s1}^*(2860)$ and $D_{s3}^*(2860)$ resonances. We have completed the study with the same analysis for the $D_{s1}^*(2700)$ and $D_{sJ}(3040)$. Our theoretical results indicate that the $D_{s1}^*(2700)$, $D_{s1}^*(2860)$, $D_{s3}^*(2860)$ and $D_{sJ}(3040)$ mesons can be accommodated as the $nJ^P = 21^-$, 31^- , 13^- and 31^+ , respectively. These predictions are in agreement with other theoretical studies of the same resonances.

For this study we have used a constituent quark model which describes successfully the hadron phenomenology from light to heavy quark sectors. The 1-loop corrections to the OGE potential and the coupling of non- $q\bar{q}$ degrees of freedom in the $1^+ c\bar{s}$ channel improve the theoretical mass splittings between the $D_{s0}^*(2317)$, $D_{s1}(2460)$ and $D_{s1}(2536)$ mesons. Moreover, the decay properties of the $D_{s1}(2536)$ and $D_{s2}(2573)$ are well reproduced. It is worth to mention that the strong decays have been calculated using an adapted version of the 3P_0 decay model in which the strength γ of the decay interaction depends on the mass scale through the reduced mass of the quark-antiquark in the decaying meson.

Finally, there are states still undiscovered by experiments in the mass energy region of the $D_{s1}^*(2700)$, $D_{sJ}^*(2860)$ and $D_{sJ}(3040)$ mesons. We have provided the masses and strong decay properties of those which belong to the same spin-multiplets. We hope that this study will help experimentalists in carrying out a search for them.

ACKNOWLEDGMENTS

This work has been partially funded by Ministerio de Ciencia y Tecnología under Contract no. FPA2013-47443-C2-2-P, by the European Community-Research Infrastructure Integrating Activity ‘‘Study of Strongly Interacting Matter’’ (HadronPhysics3 Grant no. 283286) and by the Spanish Ingenio-Consolider 2010 Program

CPAN (CSD2007-00042). JS acknowledges financial support from a postdoctoral IUFFyM contract of the Universidad de Salamanca.

- [1] J. Beringer et al. (Particle Data Group), Phys. Rev. **D86**, 010001 (2012).
- [2] B. Aubert et al. (BaBar Collaboration), Phys. Rev. Lett. **97**, 222001 (2006).
- [3] J. Brodzicka et al. (Belle Collaboration), Phys. Rev. Lett. **100**, 092001 (2008).
- [4] B. Aubert et al. (BaBar Collaboration), Phys. Rev. **D80**, 092003 (2009).
- [5] E. S. Swanson, Phys. Rept. **429**, 243 (2006).
- [6] J. L. Rosner, J. Phys. **G34**, 127 (2007).
- [7] E. Klempt and A. Zaitsev, Phys. Rept. **454**, 1 (2007).
- [8] P. Colangelo, F. De Fazio, F. Giannuzzi, and S. Nicotri, Phys. Rev. **D86**, 054024 (2012).
- [9] R. Aaij et al. (LHCb collaboration), Phys. Rev. Lett. **113**, 162001 (2014).
- [10] R. Aaij et al. (LHCb collaboration), Phys. Rev. **D90**, 072003 (2014).
- [11] Q.-T. Song, D.-Y. Chen, X. Liu, and T. Matsuki (2014), arXiv:1408.0471 [hep-ph].
- [12] Z.-G. Wang (2014), arXiv:1408.6465 [hep-ph].
- [13] S. Godfrey and K. Moats, Phys. Rev. **D90**, 117501 (2014).
- [14] D. Zhou, E.-L. Cui, H.-X. Chen, L.-S. Geng, X. Liu, et al., Phys. Rev. **D90**, 114035 (2014).
- [15] H.-W. Ke, J.-H. Zhou, and X.-Q. Li (2014), arXiv:1411.0376 [hep-ph].
- [16] Q.-T. Song, D.-Y. Chen, X. Liu, and T. Matsuki (2015), arXiv:1501.03575 [hep-ph].
- [17] J. Segovia, D. Entem, and F. Fernandez, Phys. Lett. **B715**, 322 (2012).
- [18] J. Vijande, F. Fernandez, and A. Valcarce, J. Phys. **G31**, 481 (2005).
- [19] A. Valcarce, H. Garcilazo, F. Fernandez, and P. Gonzalez, Rept. Prog. Phys. **68**, 965 (2005).
- [20] J. Segovia, D. Entem, F. Fernandez, and E. Hernandez, Int. J. Mod. Phys. **E22**, 1330026 (2013).
- [21] F. Fernandez, A. Valcarce, P. Gonzalez, and V. Vento, Phys. Lett. **B287**, 35 (1992).
- [22] H. Garcilazo, A. Valcarce, and F. Fernandez, Phys. Rev. **C63**, 035207 (2001), *ibid.* Phys. Rev. **C64**, 058201 (2001).
- [23] J. Vijande, H. Garcilazo, A. Valcarce, and F. Fernandez, Phys. Rev. **D70**, 054022 (2004).
- [24] J. Segovia, A. Yasser, D. Entem, and F. Fernandez, Phys. Rev. **D78**, 114033 (2008).
- [25] J. Segovia, A. Yasser, D. Entem, and F. Fernandez, Phys. Rev. **D80**, 054017 (2009).
- [26] J. Segovia, D. Entem, and F. Fernandez, Phys. Rev. **D83**, 114018 (2011).
- [27] J. Segovia, D. R. Entem, and F. Fernandez, Phys. Rev. **D91**, 014002 (2014).
- [28] J. Segovia, D. Entem, and F. Fernandez, Phys. Lett. **B662**, 33 (2008).
- [29] E. Hiyama, Y. Kino, and M. Kamimura, Prog. Part. Nucl. Phys. **51**, 223 (2003).
- [30] D. Mohler and R. Woloshyn, Phys.Rev. **D84**, 054505 (2011), 1103.5506.
- [31] S. Godfrey and N. Isgur, Phys.Rev. **D32**, 189 (1985).
- [32] O. Lakhina and E. S. Swanson, Phys.Lett. **B650**, 159 (2007), hep-ph/0608011.
- [33] S. Gupta and S. Radford, Phys.Rev. **D24**, 2309 (1981).
- [34] L. Micu, Nucl. Phys. **B10**, 521 (1969).
- [35] A. Le Yaouanc, L. Oliver, O. Pène, and J. C. Raynal, Phys. Rev. **D8**, 2223 (1973).
- [36] A. Le Yaouanc, L. Oliver, O. Pène, and J.-C. Raynal, Phys. Rev. **D9**, 1415 (1974).
- [37] J. Ferretti and E. Santopinto, Phys. Rev. **D90**, 094022 (2014), 1306.2874.
- [38] J. Segovia, Ph.D. thesis, Universidad de Salamanca (2012), <http://inspirehep.net/record/1316438>.
- [39] E. Ackleh, T. Barnes, and E. Swanson, Phys. Rev. **D54**, 6811 (1996), hep-ph/9604355.
- [40] S. Okubo, Phys. Lett **5**, 165 (1963).
- [41] G. Zweig, CERN-TH-412, NP-8419 (1964).
- [42] J. Iizuka, Progress of Theoretical Physics Supplement **37**, 21 (1966).
- [43] J. Segovia, C. Albertus, D. Entem, F. Fernandez, E. Hernandez, et al., Phys. Rev. **D84**, 094029 (2011), 1107.4248.
- [44] J. Segovia, C. Albertus, E. Hernandez, F. Fernandez, and D. Entem, Phys. Rev. **D86**, 014010 (2012), 1203.4362.